Influence of water vapour on 316L oxidation at high temperature - in situ X-Ray diffraction

Henri Buscail, Raphaël Rolland, Sébastien Perrier

INFLUENCE OF WATER VAPOUR ON 316L OXIDATION AT HIGH TEMPERATURE - *IN SITU* X-RAY DIFFRACTION

Henri BUSCAIL[a], Raphaël ROLLAND[a], Sébastien PERRIER[a]

[a] Université de Clermont Auvergne, LVEEM, 8 rue J.B. Fabre, 43009 Le Puy-en-Velay, France

Abstract – Water vapour mixed with air (10 vol.% H_2O) has little effect on the AISI 316L stainless steel oxidation under isothermal conditions at 800 and 900 °C. The oxide scale is composed of Cr_2O_3 and $Mn_{1.5}Cr_{1.5}O_4$ located at the external interface. Results show that the presence of water lowers the specimen's mass gain. At 1000 °C, the effect of water vapour on the scale structure is deleterious. *In situ* X-ray diffraction permits to show that the breakaway is due to iron oxidation starting after about 30 hours. This leads to an external Fe_2O_3 scale growth and an internal multilayered $FeCr_2O_4$ scale formation.

Résumé – L'air contenant 10 vol.% H_2O a peu d'effet sur l'oxydation de l'alliage AISI 316L à 800 et 900°C. La couche d'oxyde est alors constituée de Cr_2O_3 et de $Mn_{1.5}Cr_{1.5}O_4$ qui est situé à l'interface externe. Les résultats montrent que la présence de vapeur d'eau diminue la vitesse de prise de masse. A 1000 °C la vapeur d'eau a un effet désastreux sur la structure de la couche d'oxyde. La diffraction des rayons X *in situ* à 1000°C sous air humide a permis de montrer que l'oxydation du fer débute après environ 30 heures d'oxydation. Ceci conduit à la formation d'une couche externe de Fe_2O_3 et une couche interne stratifiée de $FeCr_2O_4$.

1. INTRODUCTION

The AISI 316L austenitic stainless steel is widely used in industrial applications due to its good creep properties and oxidation resistance provided by the high alloy chromium content [1-8]. Several studies proposed that, at high temperature, chromia-forming alloys such as AISI 316L SS exhibit an oxide growth leading mainly to Cr_2O_3 and $Mn_{1.5}Cr_{1.5}O_4$ formation [9-11]. It has also been demonstrated that yttria addition leads to an increased oxidation resistance at 800°C [12]. The role of molybdenum on the AISI 316L oxidation mechanism has been already discussed. It has been demonstrated that molybdenum plays a similar protective role as the one provided by silicon. In dry air, it hinders iron oxidation and leads to a better keying of the chromia scale in the alloy [13-15]. Water vapour is present in many industrial gases. It is a constituent of combustion gases and can affect high temperature corrosion of heat exchangers or engines. Many investigations have been conducted to increase solid oxide fuel cells performance and increase the corrosion resistance of metallic interconnects [16, 17].

Tirés à part : H. BUSCAIL, LVEEM, 8 rue J.B. Fabre, CS 10219, 43009 Le Puy en Velay, France

Water vapour is also present in power-generation systems and increasing service temperatures leads to corrosion problems. Water vapour effects have already been described in the literature [18-21]. Several studies were conducted on chromia forming alloys [22-26]. Generally, water vapour has a major effect on the growth rate of oxide scales. Increasing the amount of water vapour in the atmosphere reduces the time to the onset of breakaway oxidation [27]. Galerie et al. have explained that the breakaway on a Fe-15%Cr alloy was induced by rapid growth of hematite at the metal/chromia interface, at 800-1000 °C, in Ar-15 vol.% H_2O [23]. But in many cases, the chromia scale failure was related to the formation of the $CrO_2(OH)_2$ and $Cr(OH)_3$ volatile hydroxides [28-30]. Evaporation can lead to the alloy chromium depletion resulting in the formation of an iron-rich non-protective scale. Young proposed that water vapour affects chromia scale growth similarly to what is observed with reactive metal elements [31]. Both segregate to oxide grain boundaries. Grain boundary cation diffusion is then largely suppressed increasing the oxygen internal diffusion and refining the oxide grain structure. On the other hand, he also explained that in short-term laboratory experiments at temperatures above 800 °C, chromium volatilization could usually be neglected, even in O_2/H_2O gas mixtures. Refining of the oxide grain structure under wet conditions has also been observed by Jacob et al. after pure chromium oxidation [32]. Recently, Othman et al. proposed that water vapour has no significant effect if a large chromium reservoir induces the growth of a continuous Cr_2O_3-scale layer [33]. The ability of Fe–Cr alloys to form a protective oxide scale was related to the chromium concentration at the alloy surface. When the concentration of chromium is too low, iron-rich oxides form, inducing breakaway oxidation. Rahmel et al. suggested that an H_2/H_2O gas mixture can be formed in voids within the scale then facilitating rapid inward transport of oxygen [18]. From the literature review it can be stated that owing to its relatively high chromium content and alloying elements, AISI 316L is oxidation resistant at temperatures up to 1000 °C in dry environments and in isothermal conditions.

The aim of the present work is to determine the effect of water vapour on the oxidation mechanism of the AISI 316L alloy compared with dry air experiments. *In situ* X-ray diffraction with flowing moist air (10 vol.% H_2O) will provide useful information on the oxidation process at operating temperatures. It will be determined if a change in the structural composition of the layer occurs during the oxidation test and if any oxide phase transitions occur during cooling to room temperature.

2. EXPERIMENTAL

The material used in the present work is an AISI 316L austenitic stainless steel. The alloy composition is given in *table I*. The specimens, provided by APERAM Alloys Imphy, were polished on SiC paper up to 800 grade, then washed with ethanol and finally dried prior to isothermal oxidation at 800, 900 and 1000°C. The specimens are 1.5 mm thick and show a total surface area of about 6 cm^2.

The kinetic results obtained under isothermal conditions were recorded during 96 h using a Setaram TG-DTA 92-1600 microthermobalance. The *in situ* characterization of the oxide scales was carried out in a high temperature MRI chamber adapted on an X-ray Philips X' PERT MPD diffractometer (Copper radiation, $\lambda_{K\alpha}$ = 0.154 nm). The diffraction patterns are registered every hour at 1000 °C in 10 vol.% H_2O flowing air.

X-ray diffraction (XRD) conditions were: Θ–2Θ scan, step 0.02°, range from 10 to 80°, 3 s counting time. The morphology of the external interface as well as the cross sections was observed using a Scanning Electron Microscope (SEM) JEOL JSM-7600F. The analysis of the scale was performed with a LINK energy dispersive X-ray spectroscopy (EDXS). The EDXS point analyses were performed with an electron probe focused to 1 µm spot. The water vapour experiments were performed in air containing 10 vol.% H_2O. The flowing air (8 L/h flow rate) is saturated through

boiling water. Then, the water bath humidifier maintained at 50 °C controls the water vapour ratio by condensation of the excess water vapour. All the connecting tubes are maintained at 100°C in order to avoid any water condensation out of the furnaces. A schematic drawing of the rig has been provided in a previous paper [34]. Similar gas humidifiers were used either for TGA and wet *in situ* DRX (MRI chamber). Dry air testing was performed in flowing air at atmospheric pressure. The weight change of the samples was determined after each oxidation test on a balance with an accuracy of 0.01 mg.

Table I. Composition of the AISI 316L SS (weight %)

AISI 316L	**Fe**	**Cr**	**Ni**	**Mo**	**Mn**	**Si**	**C**
Content	Balance	17.7	10.9	2.16	1.57	0.55	0.023

3. RESULTS

3.1. Isothermal kinetics

The mass gain curves per unit area are given in *figure 1*. All isothermal thermogravimetric analyses were carried out during 96 h at 800, 900 and 1000 °C in ambient air and wet air (10 vol.% H_2O). A parabolic regime was observed throughout the 96 h oxidation tests except when testing at 1000 °C in wet air. The k_p values are given in *table II*. At 800 °C, the oxidation rates are similar under dry and wet air. At 900 °C, the oxidation rate is slightly higher in dry air than in wet air. At 1000 °C, a parabolic regime is followed in dry air whereas in wet air, 10 vol.% water vapour induces an important increase of the oxidation rate after 30 hours oxidation. At 1000 °C, the oxidation rate recorded before the breakaway regime is similar in wet air and dry air. An apparent activation energy (E_a) was calculated from the slope of the Arrhenius plots of the k_p values, E_a = 208 ± 30 kJ mol^{-1} under dry conditions and E_a = 241 ± 30 kJ mol^{-1} in wet air.

Table II . k_p values obtained on the AISI 316L SS after dry air and wet air (10 vol.% H_2O) oxidation between 800 at 1000 °C.

Temperature	**k_p (g^2 cm^{-4} s^{-1}) Dry air**	**k_p (g^2 cm^{-4} s^{-1}) Wet air**
800°C	$4.8 \pm 0.1\ 10^{-14}$	$3.5 \pm 0.1\ 10^{-14}$
900°C	5.8 ± 0.110^{-13}	$2.6 \pm 0.1\ 10^{-13}$
1000°C	$1.9 \pm 0.1\ 10^{-12}$	$2.5 \pm 0.1\ 10^{-12}$ (before 24h)

3.2. Scale morphology

SEM examinations were carried out on the specimen cross section (*figure 2*) in order to identify the elements constituting the oxide scale. After 96 h oxidation in dry and wet air at 800, 900 and in dry air at 1000 °C, the scale is adherent. EDXS analyses performed on the cross section show that manganese chromite is located at the scale/gas interface. The middle part of the oxide scale is mainly composed of chromia. Some internal silicon oxidation is observed along the alloy grain boundaries at temperatures higher than 800 °C. No influence of water vapour is observed on

Tirés à part : H. BUSCAIL, LVEEM, 8 rue J.B. Fabre, CS 10219, 43009 Le Puy en Velay, France

the silicon internal oxidation process. Nevertheless, it appears that in wet air the oxide scale is more convoluted. At 1000 °C, in wet air, the outer scale corresponds to hematite. This oxide subscale spalled off during cooling to room temperature (30 °C/minute) and is not observed on the cross section. The inner scale is multilayered and shows alternatively $FeCr_2O_4$ scales and non-oxidized nickel-rich metallic layers. EDXS analyses performed in the metallic substrate, under the oxide scale, show that in the upper 2 µm depth the chromium content is 14.2 ± 0.3 wt.%. The 17.7 wt.% bulk content is reached at 15 µm deep inside the alloy. The alloy chromium ratio close to the interface is the same whatever the temperature and gaseous environment. It then appears that water vapour does not lead to important chromium depletion inside the metallic substrate.

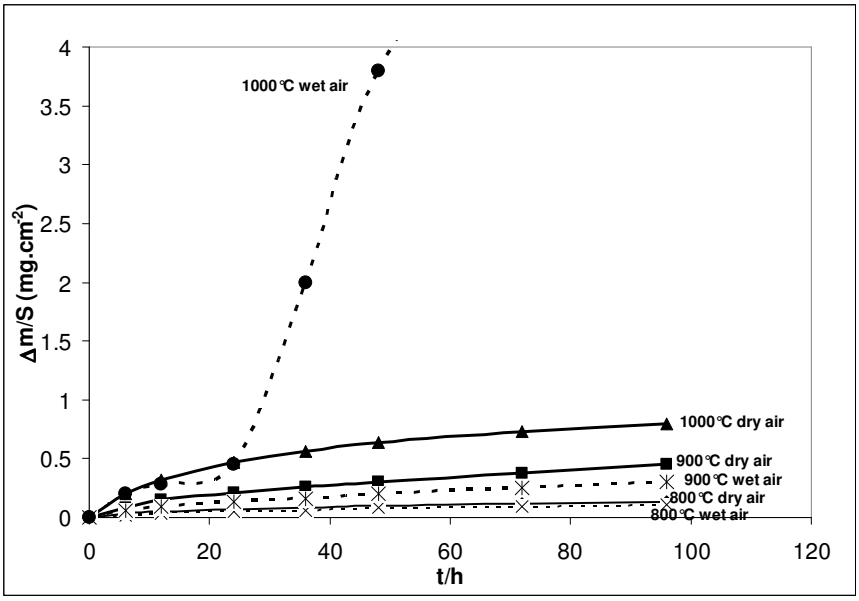

Figure 1. Mass gain curves obtained after 96h isothermal oxidation of AISI 316L SS under dry air and wet air (10 vol.% H_2O) at 800, 900 °C, and 1000°C.

3.3. X-Ray Diffraction results after isothermal oxidation

XRD patterns obtained from the AISI 316L SS sample after 96 h isothermal oxidation at 800, 900, 1000 °C in dry air reveal the presence of $Mn_{1.5}Cr_{1.5}O_4$ (JCPDS 33-0892) and Cr_2O_3 (JCPDS 38-1479) after oxidation at all temperatures. The relative intensity of the alloys peaks is smaller at 1000 °C due to the higher oxide thickness. After wet air oxidation, $Mn_{1.5}Cr_{1.5}O_4$ and Cr_2O_3 are present on the alloy surface after oxidation at 800 and 900°C. At 1000°C, XRD analysis of the remaining oxide only shows the presence of $FeCr_2O_4$ (JCPDS 34-0140) because the external Fe_2O_3 scale totally spalled off during cooling at 30°C/minute. Fe_2O_3 scale pieces have found fallen down out of the crucible.

3.4. *In situ* X-Ray Diffraction results in wet air at 1000°C

The oxide scale formed on AISI 316L was analysed by *in situ* XRD on the metallic substrate at 1000°C, in wet air (10 vol.% H_2O) during 65 hours. *Figure 3* shows the presence of the $Mn_{1.5}Cr_{1.5}O_4$ (JCPDS 33-0892) and Cr_2O_3 (JCPDS 38-1479) during the 30 first hours of oxidation. It appears that both oxides nucleate simultaneously on the specimen surface during the first hour of oxidation and remain present together on the surface. No other oxides were formed during the 30 first hour oxidation. After 36 hours oxidation, hematite Fe_2O_3 (JCPDS 24-0027) is detected on the

alloy surface and Cr_2O_3 peaks are still observed. After 65 hours oxidation, the hematite scale is thick and the $FeCr_2O_4$ inner oxide is hardly detected. After cooling to room temperature, *figure 3* shows that the XRD pattern obtained does not show the presence of hematite anymore. $FeCr_2O_4$ and the alloy are the only phases observed on the diffraction pattern due to the complete hematite scale spallation during cooling. *In situ* XRD results at 1000°C, in dry air, were already presented in a previous paper [13]. It was shown that $Mn_{1.5}Cr_{1.5}O_4$ and Cr_2O_3 were detected on the alloy surface all along the oxidation test in dry air and after cooling to room temperature.

4. DISCUSSION

Kinetic results have been obtained on AISI 316L between 800 at 1000 °C under isothermal conditions (*figure 1*). The parabolic behaviour was always followed in this temperature range under dry conditions and under wet conditions at 800 and 900 °C. This permitted the calculation of the parabolic rate constants k_p at each temperature (*table II*). The parabolic rate constant at 1000 °C in moist air was calculated from the kinetic curve obtained before 24 hours oxidation. At 1000 °C, in dry air, the k_p value is calculated from the data obtained during 96 h oxidation. An apparent activation energy (E_a) was calculated from the slope of the Arrhenius plots of the k_p values, E_a = 208 ± 30 kJ mol^{-1} under dry conditions and E_a = 241 ± 30 kJ mol^{-1} in wet air. These values are close to the one generally proposed in the literature when Cr_2O_3 is formed on the alloys in this temperature range [32, 35].

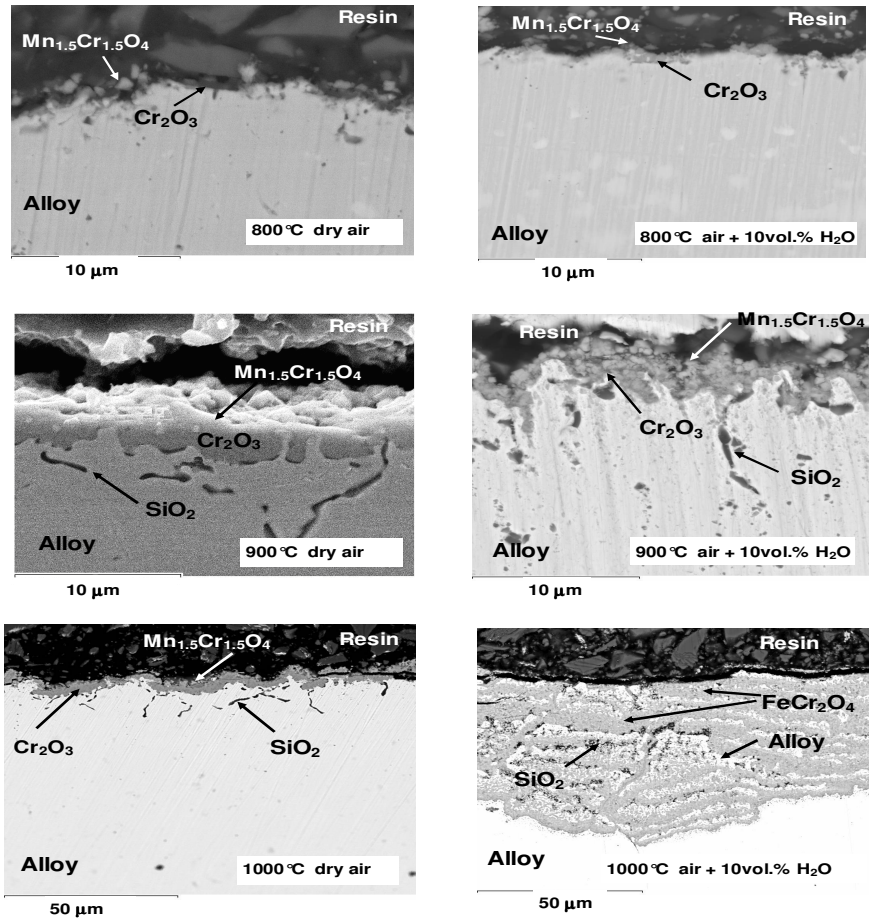

Figure 2. SEM cross-section on the AISI 316L SS oxidized at 800, 900, 1000°C in dry air or wet air (10 vol.% H_2O) for 96 h.

Tirés à part : H. BUSCAIL, LVEEM, 8 rue J.B. Fabre, CS 10219, 43009 Le Puy en Velay, France

The apparent activation energies are in good agreement with the SEM cross-section observation (*figure 2*) showing that the scale was mainly composed of a continuous chromia scale, acting as a diffusion barrier. According to SEM and XRD analyses, the good kinetic behaviour at 800 and 900°C, in dry and moist air, appears to be mainly due to the absence of iron containing oxides in the scale. *Figure 1* also shows that water vapour slightly decreases the oxidation rate relative to those registered in dry conditions and the apparent activation energy is higher in wet air. As proposed by other authors it could be due to weight losses related to the formation of the volatile hydroxide $CrO_2(OH)_2$ [28-30]. At 1000 °C, the scale remains protective during the oxidation test in dry air, (*figure 1 and figure 2*). $Mn_{1.5}Cr_{1.5}O_4$ and Cr_2O_3 are present all along the oxidation test. In wet air, oxidation at 1000 °C firstly leads to $Mn_{1.5}Cr_{1.5}O_4$ and Cr_2O_3 formation. Nevertheless, breakaway corrosion occurred after 30 hours oxidation. *In situ* X-ray diffraction permit to analyse the oxides formed on AISI 316L during isothermal oxidation at 1000 °C in moist air (*figure 3*). The breakaway oxidation is due to the iron oxidation starting after 30 hours oxidation. This leads to an external hematite scale growth and an internal multilayered $FeCr_2O_4$ scale formation.

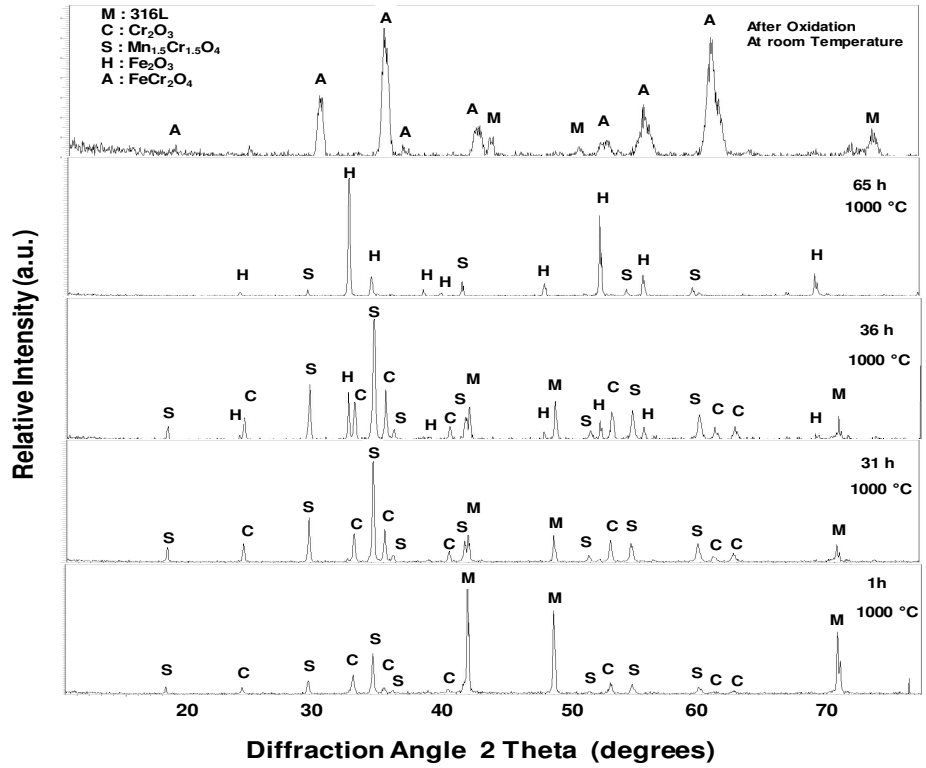

Figure 3. *In situ* XRD patterns obtained during the oxidation of the 316L alloy at 1000°C under wet air (10 vol.% H_2O).

Some authors have observed that water vapour can induce a breakaway during high temperature oxidation of iron-based chromia-forming alloys [20, 23]. Then, it was observed that it depends upon the oxidation time, testing conditions and the chromium alloy content [23]. As discussed above, chromium volatilization by formation oxy-hydroxides $CrO_2(OH)_2$ can be envisaged [36, 37]. Some authors also envisaged the transport of H_2O into the oxide scale by the diffusion of hydrogen as H^+, OH^- or H_2O in the oxide scale [38, 39]. In this study, manganese chromite and chromia were observed during the initial oxidation stage at 1000°C under wet air. Nevertheless, after about 30 hours oxidation, the protective chromia scale fails and breakaway appeared. It is proposed that water dissociation occurred on the specimen surface [23, 40]. This

dissociation is more important at 1000 °C than at lower temperature because water dissociation is endothermic. Then, the diffusion of hydrogen-containing species could occur. Transport of H_2O into the oxide scales is performed by the incorporation of hydrogen in the form of H^+ or H_2O [38, 39, 41]. It is assumed that protons (H^+) from water vapour might dissolve in the oxides and diffuse at grain boundaries. Essuman et al. proposed a model to explain the internal oxidation of chromium alloys [20, 21]. Ardigo et al. performed gold and deuterium marking experiments and have evidenced that Fe_3O_4 and Cr_2O_3 scales are permeable to hydrogen [42]. The low H^+ and OH^- radii permit their diffusion through the oxide scale. Then, the increase of protons in the scale changes the oxide defect chemistry and could be responsible for the change in the growth mechanism. It can then be considered that the reaction of H^+ (and/or H_2O) with the metallic substrate under the chromia scale form H_2 and wüstite [36, 37]. Thermodynamic data indicate that, at 1000 °C, wüstite is more stable than H_2O. Mikkelsen et al. also explained that addition of water vapour favours the formation of wüstite [43]. When FeO and chromia are present together they react to form $FeCr_2O_4$ wich explains that wüstite does not accumulate at the internal interface and is not detected by XRD [44]. As observed by *in situ* XRD (*figure 3*), iron ions also diffuse through the scale to form Fe_2O_3 at the external interface, then inducing the breakaway oxidation.

5. CONCLUSION

In situ X-ray diffraction was used to identify the oxides formed on the AISI 316L stainless steel during isothermal oxidation at 1000 °C in moist air (10 vol.% H_2O). Our results show the presence of the $Mn_{1.5}Cr_{1.5}O_4$ and Cr_2O_3 chromia growing simultaneously on the specimen surface before 30 hours oxidation. After about 30 hours oxidation, Fe_2O_3 is growing on the specimen surface at the external interface and internal corrosion leads to a multilayered $FeCr_2O_4$ scale. Hematite, located at the external interface, spalled off easily during cooling to room temperature. Water vapour clearly promots iron oxidation at 1000°C. At 800 and 900°C, 10 vol.% H_2O in air has no detrimental effect on the AISI 316L stainless steel isothermal oxidation. The oxide scale is always composed of Cr_2O_3 with a small amount of $Mn_{1,5}Cr_{1,5}O_4$ at the external interface. The lower oxidation rate can be related to chromia evaporation in wet air.

6. REFERENCES

[1] J.E. Indacochea, J.L. Smith, K.R. Litko, E.J. Karell, A.G. Raraz, Oxid. Met. (2001) 55 1-15.
[2] A.L. Johnson, D. Parsons, J. Manzerova, D.L. Perry, D. Koury, B. Hosterman, J.W. Farley, J. Nuc. Mat. 328 (2004) 88-96.
[3] J. Pitter, F. Cerny, J. Cizner, J. Suchanek, D. Tischler, Surf. Coat. Tech. 200 (2005) 73-76.
[4] A.A. Syed, T.A. Denoirjean, P. Fauchais, J.C. Labbe, Surf. Coat. Tech. 20 (2006) 4368-4382.
[5] C. Vernault, J. Mendez, Ann. Chim. Sci. Mat. 24 (1999) 351-362.
[6] X. Wang, L.F. Wang, M.L. Zhu, J.S. Zhang, M.K. Lei, Trans. Nonferrous Met. Soc. China 16 (2006) s676-s680.
[7] Seung-Goo Kim, Ming-Zhi Hong, Sung Pil Yoon, Jonghee Han, Suk Woo Nam, Tae Hoon Lim, Seong-Ahn Hong, J. Sol-Gel Sci. Tech. 28 (2003) 297-306.
[8] A.V.C. Sobral, M.P. Hierro, F.J. Pérez, W. Ristow Jr., C.V. Franco, Mater. Corros. 51 (2000) 791-796.
[9] Raghuvir Singh, Narendra B. Dahotre, J. Mat. Sci. 40 (2005) 5619-5626.
[10] P.N.S. Stokes, F.H. Stott, G.C. Wood, Mat. Sci. Engi. A121 (1989) 549-554.
[11] A. Bautista, F. Velasco, M. Campos, M.E. Rabanal, J.M. Torralba, Oxid. Met. 59 (2003) 373-393.

Tirés à part : H. BUSCAIL, LVEEM, 8 rue J.B. Fabre, CS 10219, 43009 Le Puy en Velay, France

[12] A. Bautista, F. Velasco, J. Abenojar, Corros. Sci. 45 (2003) 1343-1354.
[13] H. Buscail, S. El Messki, F. Riffard, S. Perrier, R. Cueff, E. Caudron, C. Issartel, Mat. Chem. Phys., 111 (2008) 491-496.
[14] H. Buscail, S. El Messki, F. Riffard, S. Perrier, R. Cueff, C. Issartel, J. Mat. Sci. 43 (2008) 6960-6966.
[15] H. Buscail, S. El Messki, F. Riffard, S. Perrier, C. Issartel, Oxid. Met. 75 (2011) 27-39.
[16] L. Antoni, Mater. Sci. Forum 461–464 (2004) 1073-1090.
[17] S. Fontana, S. Chevalier, G. Caboche, J. Power Sources 193 (2009) 136-145.
[18] A. Rahmel, J. Tobolski, Corros. Sci. 5 (1965) 333-346.
[19] H. Buscail, S. Heinze, P. Dufour, J.P. Larpin, Oxid. Met. 47 (1997) 445-464.
[20] E. Essuman, G.H. Meier, J. Zurek, M. Hänsel, L. Singheiser, W.J. Quadakkers, Scripta Materialia, 57 (2007) 845-848.
[21] E. Essuman, G.H. Meier, J. Zurek, M. Hänsel, T. Norby, L. Singheiser, W.J. Quadakkers, Corros. Sci. 50 (2008) 1753-1760.
[22] D.L. Douglass, P. Kofstad, A. Rahmel, G.C. Wood, Oxid. Met. 45 (1996) 529-621.
[23] A. Galerie, S. Henry, Y. Wouters, M. Mermoux, J.P. Petit, L. Antoni, Mater. High Temp. 22 (2005) 105-112.
[24] G.R. Holcomb, D.E. Alman, Scripta Materialia 54 (2006) 1821-1825.
[25] Y. Wouters, G. Bamba, A. Galerie, M. Mermoux, J.P. Petit, Mater. Sci. Forum 461–464 (2004) 839-846.
[26] H. Asteman, J.E. Svensson, L.G. Johansson, Oxid. Met. 57 (2002) 193-216.
[27] Shen Jianian, Zhou Longjiang, Li Tiefan, Oxid. Met. 48 (1997) 347-356.
[28] E.J. Opila, Mater. Sci. Forum 461-464 (2004) 765-774.
[29] X. Peng, J. Yan, Y. Zhou, F. Wang, Acta Materialia 53 (2005) 5079-5088.
[30] M. Schütze, D. Renusch, M. Schorr, Mater. High Temp. 22 (2005) 113-120.
[31] D.J. Young, Mater. Sci. Forum 595-598 (2008) 1189-1197.
[32] Y.P. Jacob, V.A.C. Haanappel, M.F. Stroosnijder, H. Buscail, P. Fielitz, G. Borchardt, Corros. Sci. 44 (2002) 2027-2039.
[33] N.K. Othman, N. Othman, J. Zhang, D.J. Young, Corros. Sci. 51 (2009) 3039-3049.
[34] R. Rolland, C. Issartel, S. Perrier, H. Buscail, Corros. Engi., Sci. Technol. 46 (2011) 634-641
[35] J.H. Chen, P.M. Rogers, J.A. Little, Oxid. Met. 47 (1997) 381-410.
[36] N.K. Othman, N. Othman, J. Zhang, D.J. Young, Corros. Sci. 51 (2009) 3039-3049.
[37] N.K. Othman, J. Zhang, D.J. Young, Corros. Sci. 52 (2010) 2827-2836.
[38] A. Galerie, Y. Wouters, M. Caillet, Mater. Sci. Forum, 369-370 (2001) 231-238.
[39] T. Norby, Amer. Ceram. Soc. 23 (1987) 107-123.
[40] C. Issartel, H. Buscail, Y. Wang, R. Rolland, M. Vilasi, L. Aranda, Oxid. Met. 76 (2011) 127-147.
[41] T. Norby, J. de Phys. IV 3 (1993) 99-106.
[42] M.R. Ardigo, I. Popa, S. Chevalier, S. Weber, O. Heintz, M. Vilasi, Oxid. Met. 79 (2013) 495–505.
[43] L. Mikkelsen, S. Linderot, Mater. Sci. Engi. A361 (2003)198-212.
[44] K. Nagata, R. Nishiwaki, Y. Nakamura, T. Maruyama, Solid State Ionics 49 (1991)161-166.